methods

Mass spectrometric determination of apolipoprotein molecular stoichiometry in reconstituted high density lipoprotein particles[S]

John B. Massey,* Henry J. Pownall,* Stephen Macha,† Jamie Morris,§ Matthew R. Tubb,§ and R. A. Gangani D. Silva[1,§]

Section of Atherosclerosis and Vascular Medicine, Department of Medicine,* Baylor College of Medicine, Houston, TX 77030; Department of Chemistry,† Mass Spectrometry Services, University of Cincinnati, Cincinnati, OH 45221; and Department of Pathology and Laboratory Medicine,§ University of Cincinnati, Cincinnati, OH 45267

Abstract Plasma HDL-cholesterol and apolipoprotein A-I (apoA-I) levels are strongly inversely associated with cardiovascular disease. However, the structure and protein composition of HDL particles is complex, as native and synthetic discoidal and spherical HDL particles can have from two to five apoA-I molecules per particle. To fully understand structure-function relationships of HDL, a method is required that is capable of directly determining the number of apolipoprotein molecules in heterogeneous HDL particles. Chemical cross-linking followed by SDS polyacrylamide gradient gel electrophoresis has been previously used to determine apolipoprotein stoichiometry in HDL particles. However, this method yields ambiguous results due to effects of cross-linking on protein conformation and, subsequently, its migration pattern on the gel. Here, we describe a new method based on cross-linking chemistry followed by MALDI mass spectrometry that determines the absolute mass of the cross-linked complex, thereby correctly determining the number of apolipoprotein molecules in a given HDL particle. Using well-defined, homogeneous, reconstituted apoA-I-containing HDL, apoA-IV-containing HDL, as well as apoA-I/apoA-II-containing HDL, we have validated this method. The method has the capability to determine the molecular ratio and molecular composition of apolipoprotein molecules in complex reconstituted HDL particles.—Massey, J. B., H. J. Pownall, S. Macha, J. Morris, M. R. Tubb, and R. A. G. D. Silva. **Mass spectrometric determination of apolipoprotein molecular stoichiometry in reconstituted high density lipoprotein particles. *J. Lipid Res.* 2009.** 50: **1229–1236.**

Supplementary key words apolipoprotein A-I • phospholipids • cholesterol • matrix-assisted laser desorption/ionization mass spectrometry

Epidemiological studies have demonstrated that HDL-cholesterol and apolipoprotein (apo) A-I levels inversely correlate with the risk of cardiovascular disease (1, 2). Currently, there is a great deal of research interest focused on developing therapeutic methods to increase HDL-cholesterol and plasma apoA-I levels and to enhance the beneficial functional properties of HDL (3, 4). HDL complexes are heterogeneous in density, shape, size, surface charge, type of apolipoproteins present, as well as number of apolipoprotein molecules present per particle (5–7). HDL consists of ~50% protein by mass where apoA-I and apoA-II comprise 70 and 20% of the protein mass, respectively. Similar density HDL can also be separated into particles that contain only apoA-I and particles that contain both apoA-I and apoA-II (5, 6). Mature plasma spherical HDL particles may contain up to two to five molecules of apoA-I (6). Structural studies on similar diameter reconstituted discoidal (2 apoA-I/particle) and spherical (3 apoA-I/particle) HDL particles have indicated that apoA-I adopts a common organizational motif, i.e., "double belt" model, irrespective of particle shape, size, and the number of apoA-I molecules in the particle (8). In this model, two apoA-I molecules are arranged in an antiparallel fashion forming a double belt that is stabilized by salt bridge interactions (9, 10). The interaction of lipid-free apoA-I with ABCA1-expressing cells generates discoidal nascent HDL with two to four molecules of apoA-I/particle (11–13). Additionally, studies on reconstituted HDL (rHDL) demonstrate direct relationships between HDL

Abbreviations: apoA-I, apolipoprotein A-I; apoA-IV, apolipoprotein A-IV; BS^3, bis(sulfosuccinimidyl)suberate; DMPC, dimyristoyl-*sn*-glycero-3-phosphocholine; MS, mass spectrometry; M_r, molecular weight; PAGGE, polyacrylamide gradient gel electrophoresis; rHDL, reconstituted high density lipoprotein.

[1] To whom the correspondence should be addressed.
e-mail: silvar@ucmail.edu

[S] The online version of this article (available at http://www.jlr.org) contains supplementary data in the form of a figure.

This work was supported by grants from the National Institutes of Health/NHLBI to R.A.G.D.S. (K99/R00, HL-1004925) and to H.J.P. (HL-30914 and HL-56865).

Manuscript received 7 October 2008 and in revised form 21 January 2009.

Published, JLR Papers in Press, January 28, 2009.
DOI 10.1194/jlr.D800044-JLR200

size/apoA-I content and LCAT activation and cellular cholesterol transfer (10, 14, 15). Many recent in vitro studies have developed a foundation for understanding how apoA-I structure modulates HDL function and metabolism (14, 16, 17). Determination of the stoichiometry of apoA-I and other apolipoprotein molecules per HDL particle is an important component of understanding the structural basis for the metabolic functions of different HDL species.

To determine the number of apolipoprotein molecules in reconstituted rHDL particles, a technique based on chemical cross-linking followed by SDS polyacrylamide gradient gel electrophoresis (SDS-PAGGE) has been heavily used (18). According to this method, the rHDL is treated with a homobifunctional cross-linking reagent that is reactive toward the ε-amino groups of Lys residues, which generates adequate intermolecular protein cross-links to covalently join all apolipoprotein molecules within an rHDL particle. The apparent molecular weight (M_r) of the cross-linked apoA-I complex is then estimated by SDS-PAGGE in comparison to a known set of M_r standards. The apolipoprotein/particle stoichiometry is determined by dividing the estimated M_r of the cross-linked complex by the actual M_r of monomeric apoA-I. However, at low protein:cross-linker ratio, even for rHDL with two molecules of apoA-I, one sees multiple SDS-PAGGE bands due to the extent and sequence location of the intermolecular cross-links (9, 19). At high protein:cross-linker ratio, band smearing of the cross-linked complex is common, and hence the migration distance of the band is difficult to measure. The problem intensifies for rHDL particles with more than two molecules of apoA-I per particle such that determination of apolipoprotein stoichiometry per particle is somewhat speculative (20). For discoidal rHDL, the apolipoprotein stoichiometry per particle can also be estimated from the average particle diameter assuming a double belt model for the apolipoprotein and a discoidal-cylindrical shape for the particle (20). However, this method is model dependent and is not adaptable to spherical rHDL or native plasma HDL due to lack of an edge to constrain the protein. Here, we propose a new approach to determine apolipoprotein: particle stoichiometry using MALDI mass spectrometry (MS). In this method, rHDL particles are first cross-linked with a homobifunctional cross-linking reagent as required for SDS-PAGGE technique. However, instead of estimating the molecular weight by SDS-PAGGE, the absolute mass of the covalently cross-linked protein complex is determined by MALDI-MS. Our results demonstrate that this method is reliable for determining the molecular stoichiometry in differently sized rHDL particles reconstituted with a single apolipoprotein component. Moreover, our data suggest that the technique is capable of distinguishing particles and their molecular stoichiometries when two particle types are mixed together. In addition, it is applicable to rHDL particles that contain two apolipoproteins on the same particle. Hence, the MALDI-MS technique is valuable in protein stoichiometry determination in complex rHDL particles where other current techniques yield ambiguous results.

MATERIALS AND METHODS

Materials

apoA-I and apoA-II were isolated and purified from fresh human plasma as previously described (21). Recombinant apoA-IV was expressed and purified as stated before (22, 23). Dimyristoyl-*sn*-glycero-3-phosphocholine (DMPC) and POPC were from Avanti Polar Lipids (Birmingham, AL), and cholesterol, sinapic acid, and BSA were from Sigma-Aldrich Chemical Co. (St. Louis, MO). The cross-linking reagent, bis(sulfosuccinimidyl)suberate (BS^3), was from Pierce Chemical Co. (Rockford, IL).

Preparation of rHDL

Naming of rHDL particles used in the study was done using apolipoprotein and lipid used in particle reconstitution as well as native PAGGE hydrodynamic diameter of the particles (e.g., A-I-DMPC-97 represents rHDL reconstituted with apoA-I and DMPC with a 97 Å particle diameter). HDLs used in the study were reconstituted using either spontaneous solubilization of multilamellar vesicles or by Biobead-cholate removal method (9, 20, 24). See supplementary data for detailed information on different types of particle preparations. The hydrodynamic diameters of rHDL particles were determined on 8–25% native Phast gels or 4–15% Bio-Rad gels ran under native conditions using high molecular weight protein standards (GE Heathcare, Amersham; Cat. No. 17-0445-01).

Cross-linking of rHDL particles

Cross-linking of the particles was carried out as essentially described before (9). See supplementary data for details on the cross-linking procedure. Throughout the manuscript, cross-linking ratios are indicated with apolipoprotein followed by the cross-linker. Upon completion of the cross-linking reaction, protein samples were dialyzed against 10 mM ammonium bicarbonate and were lyophilized. A delipidation was carried out with two washes of chloroform:methanol at 2:1 (v/v) ratio (for 300 μg protein: 6 ml of organic solution was used) followed by a pure methanol wash. The delipidated samples were resolubilized in 10 mM ammonium bicarbonate buffer, and 50 μg aliquots were lyophilized based on a Marcwell-Lowry protein assay. The aliquots were stored at −20°C to be used in MALDI-MS analysis.

MALDI-MS measurements

The lyophilized samples were reconstituted in water to a protein concentration of 1 mg/ml, and 1 μl of this solution was combined with 2 μl of matrix for spotting on the MALDI plate. The matrix, sinapic acid, was prepared as a saturated solution of 50% acetonitirle and 1% TFA in water. The instrument used, a Bruker Daltonics Reflex-IV MALDI-TOF mass spectrometer (Billerica, MA), was optimized and calibrated using a standard BSA solution. Unmodified A-I-POPC-97 and lipid-free apoA-I were used as controls.

Determination of the number of apolipoprotein molecules per rHDL particle

In the SDS-PAGGE technique, the M_r of the most intense gel band of the 1:100 cross-linked rHDL was determined in comparison to a migration distance of a set of low molecular weight protein markers (GE Healthcare, Amersham; Cat. No. 17-0446-01). The cross-linked oligomeric M_r was then divided by the theoretical M_r of the apolipoprotein used in the particle reconstitution, which resulted in the protein molecular stoichiometry in the particle (**Table 1**). The bands correspond to the cross-linked monomeric protein under 1:100 apolipoprotein: BS^3 cross-linking conditions were not sometimes apparent on gels. Contrary, in

TABLE 1. Determination of molecular composition of rHDL particles using different approaches

Particle[a]	Starting Composition Protein/FC/PC	Number of Apolipoprotein Molecules per rHDL (n)[b]		
		Circumference Estimation	Cross-Linking[c]	MALDI-MS
AI-POPC-97[d]	1:00:78	1.9	1.9 (*1–54*) 2.5 (*2–69*)	2.0
AI-POPC-144[e]	1:09:156	2.9	4.0 (*112*)	4.0
AI-DMPC-95	1:00:210	1.8	2.5 (*69*)	2.0
AI-DMPC-126	1:11:210	2.5	3.3 (*94*)	3.0
AI-DMPC-170	1:47:420	3.5	5.1 (*143*)	4.0
AIV-DMPC-152	1:00:325	2.6	2.5 (*113*)	2.0

[a] See Materials and Methods for naming of the particles. The apoA-I/apoA-II mixed particles for which most of the above applications are not adaptable are not listed (see supplementary data for details).
[b] Refer to Materials and Methods for details on determination of number of molecules per particles using each method.
[c] The numbers in the parentheses correspond to the most prominent M_r band of cross-linked particles on SDS-PAGGE, which was used in stoichiometry determination by the SDS-PAGGE method.
[d] Two high M_r bands in SDS-PAGGE resulting from 1:10 and a:100 cross-linking of A-I-POPC-97 are presented as 1 and 2 (see Fig. 1A). For all the other rHDL particles, only the highest M_r of the cross-linked complex is given.
[e] The hydrodynamic diameters reported are for purified unmodified rHDL particles except for A-I-POPC-144, the diameter is for 1:100 cross-linked particles.

the MALDI-MS technique, the most intense, oligomeric cross-linked M_r peak in the mass spectrum of 1:100 cross-linked rHDL was divided by the mass of the internally cross-linked monomeric protein (see **Table 2**) to determine the protein stoichiometry of the particle. In the circumference estimation method, the protein stoichiometry per particle was estimated by mathematically fitting protein molecules to the circumference of rHDL particles using the following formula:

$$n = \frac{2\pi(d-10)}{1.5rh}$$

where d is the hydrodynamic diameter estimated by native PAGGE, r is the number of residues in the protein, and h is the helicity for the lipid-bound protein (20). For apoA-I, $r = 243$ and $h = 0.8$ (20). For expressed apoA-IV cleaved with Tobacco etch virus protease, $r = 377$. The helicity used for apoA-IV, 0.6 was the circular dichroism spectroscopic value reported for apoA-IV micelle complexes (25).

RESULTS

Generation and characterization of rHDL particles

We generated homogeneous discoidal rHDL particles containing either apoA-I or apoA-IV and apoA-I/apoA-II (20, 26, 27). Previously characterized, benchmark A-I-POPC-97 particles were cross-linked and analyzed side-by-side with the SDS-PAGGE and MALDI-MS techniques to determine molecular composition and to confirm the validity of the MALDI-MS method. We used the homobifunctional

TABLE 2. MALDI-MS peaks of cross-linked rHDL particles

rHDL	Protein:BS^3	Peak Location[a]				
		1 (*Monomer*)	2 (*Dimer*)	3 (*Trimer*)	4 (*Tetramer*)	(*Additional Peaks*)
A-I-unmodified	1:0	28.02 *(100)*	–*(2)*	–	–	–
AI-POPC-97	1:0	27.79 *(100)*	–*(9)*	–	–	–
	1:10	28.59 *(100)*	57.48 *(36)*	–*(7)*	–	–
	1:100	**29.70** *(19)*	**59.49*** *(100)*	–	–*(5)*	–
A-I-POPC-144	1:100	**30.00** *(9)*	59.87 *(44)*	89.95 *(17)*	**119.25*** *(100)*	–
AI-DMPC-95	1:10	28.67 *(100)*	57.71 *(72)*	–*(10)*	–*(8)*	–
	1:100	**29.45** *(23)*	**59.05*** *(100)*	–*(5)*	118.78 *(14)*	–
AI-DMPC-126[b]	1:10	28.68 *(100)*	57.59 *(50)*	86.51 *(54)*	–*(8)*	–
	1:100	**29.48** *(14)*	59.01 *(14)*	**88.52*** *(100)*	–	44.25 *(15)* (trimer/2)
AI-DMPC-170	1:10	27.87 *(100)*	55.92 *(13)*	–	–	–
	1:100	**29.49** *(5)*	59.09 *(42)*	–	**118.14*** *(100)*	–
A-IV-DMPC-152	1:0	43.28 *(100)*	86.65 *(2)*	–	–	–
	1:100	**46.00** *(34)*	**91.77*** *(100)*	–	–*(10)*	–

[a] Peak locations were manually picked from the MALDI-MS spectra. Peak intensities are presented as percentage heights (within parentheses in italics), with respect to the most intense peak in the spectrum. The locations of the "weak" peaks with intensities <10% of the most prominent M_r peak are not listed for simplicity, while their intensity contributions are listed. When there is no detectable peak in the expected location in the MALDI-MS it is denoted as "–." The highest and most intense M_r used in the determination of number of apolipoprotein molecules per rHDL particle (Table 1) is indicated by an asterisk, while the number is given in bold. The monomer peak in the 1:100 cross-linked spectrum is listed in bold irrespective of its intensity, as it was used in stoichiometry determination.
[b] The additional MALDI-MS peak present in AI-DMPC-126 (indicated by an asterisk in Fig. 2) in addition to the "expected peaks" is listed under the column labeled as Additional Peaks. This peak is the doubly charged ion of the cross-linked trimer, the most intense peak in the spectrum.

cross-linker BS^3, which has the capability of simultaneously reacting with two Lys residues and covalently joining them together, provided that the residues are within 11.4 Å, the spacer arm length of BS^3 (9). Furthermore, we have previously carried out pilot cross-linking experiments up to 5 mg/ml apoA-I rHDL to show that there are no observable interparticle cross-links that could lead to artifactual value for the protein stoichiometry (26, 27).

Mass spectrometry

MALDI-MS features one of the highest dynamic ranges for M_r detection of all MS techniques. It can detect M_r from ~1 kDa to over ~200 kDa. This range is sufficient to detect the oligomeric protein masses that result upon cross-linking even the largest native HDL particles. We took precautions to prevent falsely detecting noncovalent mass assemblies and aggregates of apolipoprotein molecules that could be misinterpreted as a single cross-linked oligomeric entity. This was done by optimizing the laser power during spectral acquisitions on commercially available BSA (theoretical M_r 66.0 kDa) and unmodified lipid-free apoA-I (theoretical M_r 28.1 kDa) until there were no significant peaks corresponding to dimer aggregates (i.e., two noncovalently bound molecules carrying a single charge, $2MH^+$). Based on several MALDI-MS spectra collected on apoA-I and BSA, we observed that the peak height ratio of $2MH^+/MH^+$ stayed <10% (Table 2). However, despite the use of sinapic acid as the MALDI matrix, which is known to generate primarily singly charged ions (MH^+), we observed low-intensity MALDI-MS peaks originated from doubly charged ions (MH^{2+}). Based on >15 independent measurements, the MALDI-MS MH^{2+}/MH^+ peak intensity ratio varied from 5–15%.

Confirmation of the number of apoA-I molecules in A-I-POPC-97 particles

Native PAGGE of A-I-POPC-97 particles indicated a homogeneous particle population of ~97 Å diameter (**Fig. 1A**). SDS-PAGGE of 1:10 and 1:100 cross-linked particles indicated a band ~28 kDa and closely spaced two high M_r bands at ~54 and~69 kDa (Fig. 1B, lane 4). The band at ~28 kDa corresponds to internally cross-linked monomeric apoA-I that did not participate in intermolecular cross-link formation. Based on the SDS-PAGGE technique, 54 and 69 kDa gel bands indicate the presence of 1.9 and 2.5 apoA-I per AI-POPC-97 particle (Table 1), highlighting the ambiguity of using this methodology (14, 19). The MALDI-MS method indicated exactly 2.0 apoA-I molecules per A-I-POPC-97 particle (Table 1). Unlike SDS-PAGGE, the MALDI-MS spectrum of 1:10 and 1:100 cross-linked A-I-POPC-97 shows two major peaks located at 28.59 and 57.48 kDa, which correspond to monomeric and dimeric apoA-I (Fig. 1C) (Tables 1, 2). Under 1:10 cross-linking conditions, the dimer band is weaker in intensity compared with that of the monomer, indicating that the cross-linker ratio is not sufficient to intermolecularly link all apoA-I molecules within a particle, as seen on SDS-PAGGE (Fig. 1B, C). At the 1:100 cross-linking ratio, the monomer band almost disappeared, indicating near total cross-linking of apoA-Is within the particles (Fig. 1B, lane 5). Another important observation seen by the MALDI-MS is the shifting of the peaks to higher masses with higher cross-linker ratios (Table 2) (and to a lesser extent, Fig. 1C). ApoA-I mass shifted from 28.59 kDa (1:10 cross-linking) to 29.70 kDa (1:100 cross-linking), reflecting an increase in the number of internal cross-linker additions to monomeric apoA-I. Based on the mass additions by the BS^3 cross-linker (138.1 Da), on average, there are approximately six cross-links in the 1:10 internally cross-linked monomeric apoA-I [(28.59–27.79) kDa/0.14 kDa ≈ 5], whereas there are ~14 cross-links in the 1:100 cross-linked monomer [(29.70–27.79) kDa/0.14 kDa ≈ 14]. The PAGGE technique is not sensitive enough to visualize these small mass shifts (**Figs. 1B, 2B**). The circumference estimation analysis carried out based on native PAGGE estimated that there are 1.9 apoA-Is per A-I-POPC-97 particle (Table 1). It is possible that the shoulder band appearing at ~70 kDa in the 1:100 cross-linked MALDI-MS spectrum (Fig. 1C) may be due to the apoA-II present in the solution as a contaminant, cross-linking to apoA-I particles (see supplementary Fig. I). This

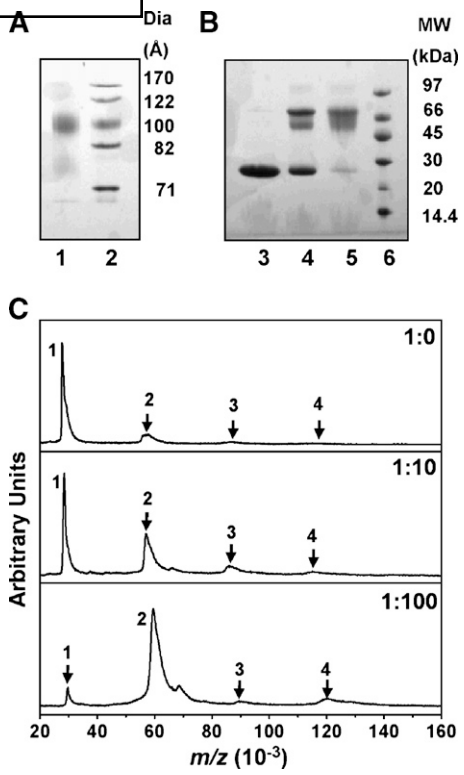

Fig. 1. Determination of the number of apoA-I molecules in an A-I-POPC-97 particle. A: 8–25% native PAGGE of A-I-POPC-97 particles (lane 1) and high molecular weight markers (lane 2). B: 8–25% SDS-PAGGE of unmodified rHDL (lane 3), rHDL cross-linked at a 1:10 and 1:100 molar ratios of apoA-I: BS^3 (lanes 4, 5, respectively). Cross-linking was carried out at 1 mg/ml apoA-I concentration. Low molecular weight standards are shown on lane 6. Gels were stained with Coomassie blue. C: MALDI mass spectra of A-I-POPC-97 rHDL cross-linked at 1:0, 1:10, and 1:100 ratios of apoA-I: BS^3. The protein-to-cross-linker ratios are indicated on each subpanel along with the expected positions of monomeric (1), dimeric (2), trimeric (3), and tetrameric (4) forms of cross-linked apoA-I. The mass accuracies of the peak positions are listed in Table 2.

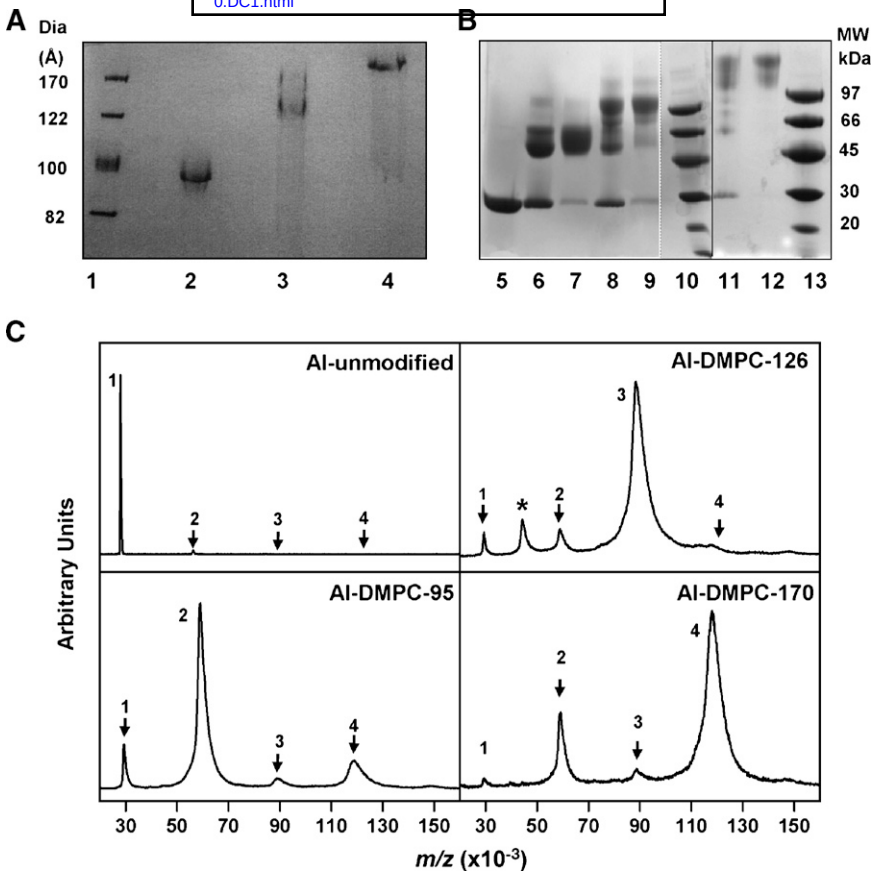

Fig. 2. Characterization of different diameter apoA-I-DMPC rHDL particles. A: 4–15% native PAGGE of A-I-DMPC rHDLs with diameters 95 Å (lane 2), 126 Å (lane 3), and 170 Å (lane 4). High molecular weight standards are on lane 1. B: 4–15% SDS-PAGGE of A-I-DMPC-95 (lanes 6, 7), A-I-DMPC-126 (lanes 8, 9), and A-I-DMPC-170 (lanes 11, 12) cross-linked with 1:10 and 1:100 ratios of A-I: BS^3, respectively. Unmodified A-I-DMPC-95 is shown for comparison (lane 5). Low molecular weight standards are on lanes 10 and 13. Merging of two different gels is indicated by a solid line, whereas unwanted lane elimination from the same gel is shown by a dashed line. Both gels were stained with Coomassie blue. C: MALDI-MS of the above particles cross-linked at a 1:100 ratio of apoA-I: BS^3. A representative spectrum of unmodified apoA-I is shown in top-left panel to indicate minimal noncovalent aggregation of apoA-I under the buffer and the instrument conditions used, which was reproducibly <10% of the unmodified apoA-I MS peak height. Labeling of expected peak positions is as in Fig. 1, while additional intense peaks are shown by an asterisk. The peak mass, percentage of intensity, and identity of each peak are listed in Table 2.

does not occur in any of the spectra of equal or larger diameter DMPC particles (see below).

Determination of apoA-I molecular stoichiometry in different diameter rHDL complexes

We generated homogeneous apoA-I-DMPC rHDL with measured diameters 95, 126, and 170 Å as analyzed by native PAGGE (Fig. 2A). The highest M_r band of the cross-linked particles moved to higher masses by SDS-PAGGE with increasing particle size, clearly indicating the increase in apoA-I molecules per particle with the increase in particle diameter (Fig. 2B). All particles under 1:10 cross-linking conditions exhibit a fraction of monomeric apoA-I that did not participate in intermolecular cross-linker formation as indicated by the band at ~28 kDa (Fig. 2, lanes 6, 8, and 11). At the 1:100 ratio, the band corresponding to monomeric apoA-I became quite faint or nondetectable due to its incorporation in intermolecular cross-links as was seen for A-I-POPC-97 above (Fig. 2B, lanes 7, 9, and 12).

A-I-DMPC-95 exhibited a similar gel migration pattern to A-I-POPC-97 on SDS-PAGGE when cross-linked with 1:10 and 1:100 (Fig. 2, lanes 6, 7; Fig. 1, lanes 4, 5). This implies that the overall particle morphology is similar when reconstituted with either lipid. The splitting of the cross-linked dimer band seen on SDS-PAGGE is an artifact of the method, as the MALDI-MS spectrum has a single peak originating from the dimer (Fig. 2C) (Table 2). Moreover, while the SDS-PAGGE method determined 2.5 apoA-I per A-I-DMPC-95, MALDI-MS determined exactly 2.0 apoA-I molecules per particle (Table 1). The peak identified in tetramer location (14%) may have a contribution from the slight contamination from the large particles, A-I-DMPC-170 in the A-I-DMPC-96 preparation, since the $2MH^+$ contribution to the spectrum is <10% (see above) (26).

For larger diameter A-I-DMPC-126 particles, the MALDI-MS indicated 3.0 apoA-Is per particle, while the SDS-PAGGE technique determined 3.4 (Tables 1, 2). In addition to the

monomer (29.48 kDa), dimer (59.01 kDa), and trimer (88.52 kDa) peaks of A-I-DMPC-126 in the MALDI-MS spectrum, there is an additional peak at 44.25 kDa indicated by an asterisk (Fig. 2) (Table 2). This peak originates from the doubly charged ion of the most intense trimer peak in the spectrum (Table 2; $3MH^{2+} = 88.52/+2 = 44.26$ kDa). Furthermore, this peak does not overlap with any other cross-linked oligomeric mass peaks in the spectrum. Hence the intensity of the ~44.25 kDa peak (which is ~15% trimer peak intensity) solely represents the contribution of doubly charged ions to the MS spectrum. As indicated above, MH^{2+}/MH^{+} vary from 5–15%. In contrast, a doubly charged ion of a most intense mass peak of a fully cross-linked rHDL, which contain an even number of apoA-I molecules, overlaps with one of its cross-linked oligomeric peaks.

Of the largest diameter particles we generated, A-I-DMPC-170 showed its highest M_r band ~143 kDa on SDS-PAGGE upon 1:100 cross-linking, implying that there are ~5.1 apoA-I molecules per particle (Table 1). Under the same cross-linking conditions, these particles generated the highest M_r peak at 118.14 kDa in MALDI-MS that determined exactly 4.0 apoA-I per particle (Tables 1, 2), whereas the circumference estimation resulted in ~3.5 apoA-I molecules. On the other hand, the larger diameter particles generated with POPC, A-I-POPC-144, were determined to have 2.9 apoA-I molecules per particle by the circumference estimation method (Tables 1, 2). However, both MALDI-MS and the SDS-PAGGE techniques determined apoA-I molecular stoichiometry to be 4.0 in these particles. Both A-I-DMPC-170 and A-I-POPC-144 MALDI-MS showed intense dimer peaks (42 and 44%, respectively), while monomer and trimer peaks were weaker in intensity (Table 2). The intensity of the dimer peak has two contributions: *a*) from the cross-linked dimers that did not form tetramers (i.e., $2MH^{+}$), and *b*) from the +2 charge state of the cross-linked tetramer (i.e., $4MH^{2+}$). Since the intensity contribution from *b*) was estimated to be ~5–15% (see above), it is reasonable to state that >25% of the peak intensity originates due to *a*). Interestingly, this data implies that dimer formation within these particles upon cross-linking is more feasible than cross-linking all four apoA-I molecules. This may be attributable to possible formation of double belt units within these large particles that contain an even number of apoA-I molecules (20). This intensity pattern was not observed for A-I-DMPC-126 with three apoA-Is.

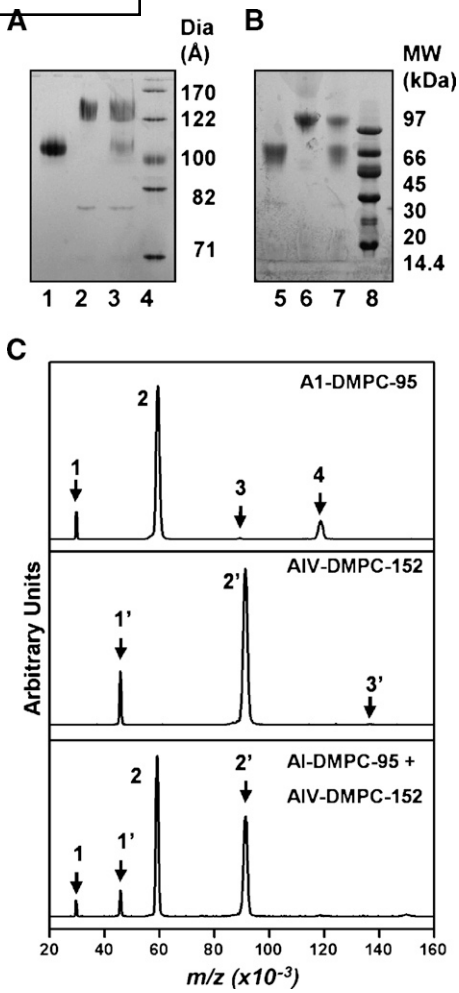

Fig. 3. Application of MALDI-MS technique to a particle mixture of apoA-IV-rHDL and apoA-I-rHDL. A: 8–25% native PAGGE of A-I-DMPC-95 (lane 1), A-IV-DMPC-152 (lane 2), and a mixture of A-I-DMPC-95 and A-IV-DMPC-152 at a 1:1 molar ratio (lane 3) along with high molecular weight standards (lane 4). B: SDS-PAGGE of A-I-DMPC-95 (lane 5), A-IV-DMPC-152 (lane 6), and the mixed particle solution in ,ane 3 cross-linked at a 1:100 ratio of protein or average protein: BS^3 (lane 7). Low molecular weight standards are shown on lane 8. Gels were processed as in Fig. 2. C: MALDI-MS spectra of the same particles and the particle mixture in B. Expected positions of cross-linked apoA-I and apoA-IV monomer, dimer, etc., are indicated as in Figs. 1 and 2, except that the apoA-IV peak positions are indicated as 1', 2', 3' for easy identification of the peaks in the mixed particle solution.

Application of the MALDI technique to complex rHDL particles

We tested the applicability of MALDI-MS method to identify rHDL particles in a mixture. For this purpose, we generated A-IV-DMPC-152 particles (**Fig. 3A**, lane 2). MALDI-MS determined exactly 2.0 apo A-IV molecules per particle (Table 1). When A-IV-DMPC-152 was mixed with A-I-DMPC-95 in a 1:1 molar ratio, the mixture does not generate rHDL particles of additional diameters (Fig. 3A, lane 3). Upon cross-linking, the gel bands corresponding to A-I-DMPC-95 and A-IV-DMPC-152 stayed the same in the mixed particle system (Fig. 3B). The MALDI-MS of cross-linked individual particles and the particle mixture indicated that this technique is capable of determining the presence of A-I-DMPC-95 and A-IV-DMPC-152 in the mixture (Fig. 3C). Our attempts of generating rHDL particles with both apoA-I and apoA-IV on the same rHDL particle were unsuccessful, perhaps corroborating with the plasma HDL data, which indicates apoA-IV resides on separate HDL particles on its own (28). Hence, to confirm that the MALDI-MS technique has the ability to identify two different apolipoproteins on the same rHDL particle, we generated mixed apoA-I/apoA-II rHDL (see supplementary Materials and Methods). These particles have similar particle diameters to A-I-POPC-97 based on PAGGE and electron microscopy (data not shown).

Upon cross-linking, the SDS-PAGGE indicates that the particles resulted in an additional gel band at ~85 kDa in addition to the band at ~69 kDa (see supplementary Fig. IB, lane 4, and compare this with Fig. 1B, lane 5). MALDI-MS of unmodified A-I/A-II-POPC-97 shows M_r peaks corresponding to unmodified apoA-I and apoA-II (see supplementary Fig. IC). As seen on SDS-PAGGE (see supplementary Fig. IB, lane 4) and MALDI-MS (see supplementary Fig. IC, bottom panel), all apoA-II incorporated into rHDL particles, and a new MALDI-MS peak that was not present in A-I-POPC-97 MALDI-MS originated at 73.56 kDa, indicating that there are indeed rHDL particles that contain two molecules of apoA-I and one molecules of dimeric apoA-II (theoretical mass 73.5 kDa). Upon using the approach *b*) on particle preparation (see supplementary Materials and Methods), the intensity of the peak at 73.56 kDa increased, indicating the presence of more apoA-I/apoA-II mixed particles compared with that of using approach *a*) (see supplementary Fig. ID). The data on mixed particles clearly indicate the applicability of the MALDI-MS technique on complex rHDL particles. The SDS-PAGGE method can be applied on such particles just for the estimation of the number of protein molecules that adds up to result in ~85 kDa. The circumference estimation method simply does not hold for stoichiometry determination of such mixed particles (Materials and Methods).

DISCUSSION

Previously, studies focused on structural details on the molecular fold of lipid free apolipoproteins, and molecular registries of lipid bound apolipoproteins have been carried out using mass spectrometric methods (8, 9, 19, 29–31). In this study, we demonstrated the feasibility of using cross-linking chemistry and MALDI-MS measurements to determine the apolipoprotein molecular stoichiometry in rHDL particles. Previous SDS-PAGGE techniques used to determine the apolipoprotein molecular stoichiometry of rHDL particles is empirical due to its relative nature of migration distance calculations, with respect to the migration distances of a set of molecular weight standards. In the SDS-PAGGE method, the accuracy of the molecular weight measurements is compromised because the cross-linked proteins migrate differently based on the extent and location of the cross-linker, and with extensive cross-linking, the gel bands become broad, making determination of the exact band location difficult (9, 19). Due to these reasons, broad multiple gel bands resulted for HDL particles containing multiple apolipoprotein molecules. On the other hand, the circumference estimation method is based on several predetermined parameters as helicity, which can vary from study to study. For example, for AIV-DMPC particles, the reported helicity values vary from 52–54% to 62% (25, 32).

When compared with SDS-PAGGE, MALDI-MS is a superior method to determine the molecular weight of oligomeric cross-linked HDL proteins. The method can accurately determine not only the M_r of the cross-linked protein oligomers, but also M_r shift of internally cross-linked monomeric protein, which was used in stochiometry determination in this method (Materials and Methods). MALDI-MS peaks have Gaussian or near-Gaussian shapes so that the peak maxima can be accurately determined with the uncertainly in hundredths decimal place when measured in kDa. The full width at half height of an average MALDI peak is ~2 kDa or less, such that the M_r of two abundant proteins more than a few kDa apart can be determined. Thus, as we have shown, it is experimentally feasible to detect differences in HDL particles that contain only apoA-I (M_r 28.1 kDa) versus those that have apoA-II (M_r 17.4 kDa) in addition to apoA-I. Moreover, other HDL proteins have a broad M_r range that is distinguishable by MALDI-MS (apoA-IV, 44.5 kDa; apoC1, 6.6 kDa; apoC2 and apo3, 8.8 kDa). In addition, BS^3 cross-linker does not dissociate under laser ionization process in MALDI-MS that could diminish the ability of data interpretations.

One potential complication inherent to the MALDI-MS method is the possibility of generating noncovalent aggregates under certain conditions and a small amount of multicharge species that contribute to the spectrum. However, our current experiments have shown that careful selection of matrix and optimization of the laser power using known standards as BSA mostly eliminate the aggregation issue (see Results). However, one should be aware of the small amount of multiply charged ions, especially doubly charged ions, that contribute to the MS spectrum (see Results).

In general, a protein stoichiometry determined for synthetic discoidal rHDL using SDS-PAGGE, MALDI-MS, and circumference estimations are in general agreement. However, in MALDI-MS, the number of apoA-I molecules per particle are determined to be exactly 2.0, 3.0, and 4.0 for different sized apoA-I only rHDL. This increased accuracy in stoichiometry mainly is due to the accuracy in determining the mass of cross-linked proteins by the MS method. Moreover, our data have clearly indicated that the technique is applicable to rHDL particle mixtures. In addition, the technique is adaptable to determine the number of protein molecules in mixed rHDL particles under which SDS-PAGE and circumference estimation methods are not applicable. Hence, the cross-linking chemistry combined with MALDI-MS is a robust method to determine the molecular protein composition of complex rHDL particles.

The authors would like to thank Cali Smith for excellent administrative assistance.

REFERENCES

1. Rader, D. J. 2006. Molecular regulation of HDL metabolism and function: implications for novel therapies. *J. Clin. Invest.* **116:** 3090–3100.
2. Barter, P. J., and K. A. Rye. 2006. The rationale for using apoA-I as a clinical marker of cardiovascular risk. *J. Intern. Med.* **259:** 447–454.
3. Barter, P., J. Kastelein, A. Nunn, and R. Hobbs. 2003. High density lipoproteins (HDLs) and atherosclerosis; the unanswered questions. *Atherosclerosis.* **168:** 195–211.

4. Joy, T., and R. A. Hegele. 2008. Is raising HDL a futile strategy for atheroprotection? *Nat. Rev. Drug Discov.* **7:** 143–155.
5. Jonas, A. 2002. Lipoprotein Structure. *In* Biochemistry of Lipids, Lipoproteins and Membranes. D. E. Vance and J. E. Vance, editors. Elsevier Science, Amsterdam. 483–504.
6. Kontush, A., and M. J. Chapman. 2006. Functionally defective high-density lipoprotein: a new therapeutic target at the crossroads of dyslipidemia, inflammation, and atherosclerosis. *Pharmacol. Rev.* **58:** 342–374.
7. Movva, R., and D. J. Rader. 2008. Laboratory assessment of HDL heterogeneity and function. *Clin. Chem.* **54:** 788–800.
8. Silva, R. A., R. Huang, J. Morris, J. Fang, E. O. Gracheva, G. Ren, A. Kontush, W. G. Jerome, K. A. Rye, and W. S. Davidson. 2008. Structure of apolipoprotein A-I in spherical high density lipoproteins of different sizes. *Proc. Natl. Acad. Sci. USA.* **105:** 12176–12181.
9. Silva, R. A., L. A. Schneeweis, S. C. Krishnan, X. Zhang, P. H. Axelsen, and W. S. Davidson. 2007. The structure of apolipoprotein A-II in discoidal high density lipoproteins. *J. Biol. Chem.* **282:** 9713–9721.
10. Martin, D. D., M. S. Budamagunta, R. O. Ryan, J. C. Voss, and M. N. Oda. 2006. Apolipoprotein A-I assumes a "looped belt" conformation on reconstituted high density lipoprotein. *J. Biol. Chem.* **281:** 20418–20426.
11. Denis, M., B. Haidar, M. Marcil, M. Bouvier, L. Krimbou, and J. Genest, Jr. 2004. Molecular and cellular physiology of apolipoprotein A-I lipidation by the ATP-binding Cassette Transporter A1 (ABCA1). *J. Biol. Chem.* **279:** 7384–7394.
12. Duong, P. T., H. L. Collins, M. Nickel, S. Lund-Katz, G. H. Rothblat, and M. C. Phillips. 2006. Characterization of nascent HDL particles and microparticles formed by ABCA1-mediated efflux of cellular lipids to apoA-I. *J. Lipid Res.* **47:** 832–843.
13. Liu, L., A. E. Bortnick, M. Nickel, P. Dhanasekaran, P. V. Subbaiah, S. Lund-Katz, G. H. Rothblat, and M. C. Phillips. 2003. Effects of apolipoprotein A-I on ATP-binding cassette transporter A1-mediated efflux of macrophage phospholipid and cholesterol: formation of nascent high density lipoprotein particles. *J. Biol. Chem.* **278:** 42976–42984.
14. Cavigiolio, G., B. Shao, E. G. Geier, G. Ren, J. W. Heinecke, and M. N. Oda. 2008. The interplay between size, morphology, stability, and functionality of high-density lipoprotein subclasses. *Biochemistry.* **47:** 4770–4779.
15. Toledo, J. D., M. A. Tricerri, B. Corsico, and H. A. Garda. 2000. Cholesterol flux between lipid vesicles and apolipoprotein AI discs of variable size and composition. *Arch. Biochem. Biophys.* **380:** 63–70.
16. Wu, Z., M. A. Wagner, L. Zheng, J. S. Parks, J. M. Shy III, J. D. Smith, V. Gogonea, and S. L. Hazen. 2007. The refined structure of nascent HDL reveals a key functional domain for particle maturation and dysfunction. *Nat. Struct. Mol. Biol.* **14:** 861–868.
17. Frank, P. G., and Y. L. Marcel. 2000. Apolipoprotein A-I: structure-function relationships. *J. Lipid Res.* **41:** 853–872.
18. Swaney, J. B., and K. O'Brien. 1978. Cross-linking studies of the self-association properties of apo- A-I and apo-A-II from human high density lipoprotein. *J. Biol. Chem.* **253:** 7069–7077.
19. Bhat, S., M. G. Sorci-Thomas, E. T. Alexander, M. P. Samuel, and M. J. Thomas. 2005. Intermolecular contact between globular N-terminal fold and C-terminal domain of ApoA-I stabilizes its lipid-bound conformation: studies employing chemical cross-linking and mass spectrometry. *J. Biol. Chem.* **280:** 33015–33025.
20. Massey, J. B., and H. J. Pownall. 2008. Cholesterol is a determinant of the structures of discoidal high density lipoproteins formed by the solubilization of phospholipid membranes by apolipoprotein A-I. *Biochim. Biophys. Acta.* **1781:** 245–253.
21. Lund-Katz, S., and M. C. Phillips. 1986. Packing of cholesterol molecules in human low-density lipoprotein. *Biochemistry.* **25:** 1562–1568.
22. Tubb, M. R., R. A. G. D. Silva, K. J. Pearson, P. Tso, M. Liu, and W. S. Davidson. 2007. Modulation of apolipoprotein A-IV lipid binding by an interaction between the N and C termini. *J. Biol. Chem.* **282:** 28385–28394.
23. Pearson, K., M. R. Tubb, M. Tanaka, X. Q. Zhang, P. Tso, R. B. Weinberg, and W. S. Davidson. 2005. Specific sequences in the N and C termini of apolipoprotein A-IV modulate its conformation and lipid association. *J. Biol. Chem.* **280:** 38576–38582.
24. Maiorano, J. N., R. J. Jandacek, E. M. Horace, and W. S. Davidson. 2004. Identification and structural ramifications of a hinge domain in apolipoprotein A-I discoidal high-density lipoproteins of different size. *Biochemistry.* **43:** 11717–11726.
25. Weinberg, R. B., and M. K. Jordan. 1990. Effects of phospholipid on the structure of human apolipoprotein A-IV. *J. Biol. Chem.* **265:** 8081–8086.
26. Davidson, W. S., and G. M. Hilliard. 2003. The spatial organization of apolipoprotein A-I on the edge of discoidal high density lipoprotein particles: a mass spectrometry study. *J. Biol. Chem.* **278:** 27199–27207.
27. Silva, R. A., G. M. Hilliard, L. Li, J. P. Segrest, and W. S. Davidson. 2005. A mass spectrometric determination of the conformation of dimeric apolipoprotein A-I in discoidal high density lipoproteins. *Biochemistry.* **44:** 8600–8607.
28. Asztalos, B. F., E. J. Schaefer, K. V. Horvath, S. Yamashita, M. Miller, G. Franceschini, and L. Calabresi. 2007. Role of LCAT in HDL remodeling: investigation of LCAT deficiency states. *J. Lipid Res.* **48:** 592–599.
29. Silva, R. A., G. M. Hilliard, J. Fang, S. Macha, and W. S. Davidson. 2005. A three-dimensional molecular model of lipid-free apolipoprotein A-I determined by cross-linking/mass spectrometry and sequence threading. *Biochemistry.* **44:** 2759–2769.
30. Bhat, S., M. G. Sorci-Thomas, R. Tuladhar, M. P. Samuel, and M. J. Thomas. 2007. Conformational adaptation of apolipoprotein A-I to discretely sized phospholipid complexes. *Biochemistry.* **46:** 7811–7821.
31. Tubb, M. R., R. A. Silva, J. Fang, P. Tso, and W. S. Davidson. 2008. A three-dimensional homology model of lipid-free apolipoprotein A-IV using cross-linking and mass spectrometry. *J. Biol. Chem.* **283:** 17314–17323.
32. Jonas, A., A. Steinmetz, and L. Churgay. 1993. The number of amphipathic alpha-helical segments of apolipoproteins A-I, E, and A-IV determines the size and functional properties of their reconstituted lipoprotein particles. *J. Biol. Chem.* **268:** 1596–1602.